Stable low-loss optical nanofibres embedded in hydrophobic aerogel

Limin Xiao,[1] M. D. W. Grogan,[1] W. J. Wadsworth,[1] R. England,[2] and T. A. Birks[1,*]

[1]*Centre for Photonics and Photonic Materials, Department of Physics, University of Bath, Bath BA2 7AY, UK*
[2]*Department of Chemical Engineering, University of Bath, Bath BA2 7AY, UK*
**t.a.birks@bath.ac.uk*

Abstract: Nanofibres, optical fibres narrower than the wavelength of light, degrade in hours on exposure to air. We show that encapsulation in hydrophobic silica aerogel (refractive index 1.05) provides protection and stability (over 2 months) without sacrificing low attenuation, strong confinement and accessible evanescent field. The measured attenuation was <0.03 dB/mm, over 10 × lower than reported with other encapsulants. This enables many nanofibre applications based on their extreme small size and strong external evanescent field, such as optical sensors, nonlinear optics, nanofibre circuits and high-Q resonators. The aerogel is more than a waterproof box, it is a completely-compatible gas-permeable material in intimate contact with the nanofibre and hydrophobic on both the macroscopic and molecular scales. Its benefits are illustrated by experiments on gas sensing (exploiting the aerogel's porosity) and supercontinuum generation (exploiting its ultra-low index).

OCIS codes: (060.2340) Fiber optics components; (060.4370) Nonlinear optics, fibers; (060.2370) Fiber optics sensors.

References and links

1. H. S. MacKenzie, and F. P. Payne, "Evanescent field amplification in a tapered single-mode optical fibre," Electron. Lett. **26**(2), 130–132 (1990).
2. J. Bures, and R. J. Ghosh, "Power density of the evanescent field in the vicinity of a tapered fiber," J. Opt. Soc. Am. A **16**(8), 1992–1996 (1999).
3. L. M. Tong, R. R. Gattass, J. B. Ashcom, S. L. He, J. Y. Lou, M. Y. Shen, I. Maxwell, and E. Mazur, "Subwavelength-diameter silica wires for low-loss optical wave guiding," Nature **426**(6968), 816–819 (2003).
4. G. Brambilla, F. Xu, P. Horak, Y. Jung, F. Koizumi, N. P. Sessions, E. Koukharenko, X. Feng, G. S. Murugan, J. S. Wilkinson, and D. J. Richardson, "Optical fiber nanowires and microwires: fabrication and applications," Adv. Opt. Photon. **1**(1), 107–161 (2009).
5. S. G. Leon-Saval, T. A. Birks, W. J. Wadsworth, P. St. J. Russell, and M. W. Mason, "Supercontinuum generation in submicron fibre waveguides," Opt. Express **12**(13), 2864–2869 (2004).
6. G. Brambilla, and D. N. Payne, "The ultimate strength of glass silica nanowires," Nano Lett. **9**(2), 831–835 (2009).
7. P. Polynkin, A. Polynkin, N. Peyghambarian, and M. Mansuripur, "Evanescent field-based optical fiber sensing device for measuring the refractive index of liquids in microfluidic channels," Opt. Lett. **30**(11), 1273–1275 (2005).
8. J. Villatoro, and D. Monzón-Hernández, "Fast detection of hydrogen with nano fiber tapers coated with ultra thin palladium layers," Opt. Express **13**(13), 5087–5092 (2005).
9. L. M. Tong, J. Y. Lou, R. R. Gattass, S. L. He, X. W. Chen, L. Liu, and E. Mazur, "Assembly of silica nanowires on silica aerogels for microphotonic devices," Nano Lett. **5**(2), 259–262 (2005).
10. Y. Li, and L. M. Tong, "Mach-Zehnder interferometers assembled with optical microfibers or nanofibers," Opt. Lett. **33**(4), 303–305 (2008).
11. D. I. Yeom, E. C. Mägi, M. R. E. Lamont, M. A. F. Roelens, L. Fu, and B. J. Eggleton, "Low-threshold supercontinuum generation in highly nonlinear chalcogenide nanowires," Opt. Lett. **33**(7), 660–662 (2008).
12. M. Sumetsky, "Basic Elements for Microfiber Photonics: Micro/Nanofibers and Microfiber Coil Resonators," J. Lightwave Technol. **26**(1), 21–27 (2008).
13. G. Vienne, Y. Li, and L. M. Tong, "Effect of Host Polymer on Microfiber Resonator," IEEE Photon. Technol. Lett. **19**(18), 1386–1388 (2007).
14. G. Brambilla, F. Xu, and X. Feng, "Fabrication of optical fibre nanowires and their optical and mechanical characterization," Electron. Lett. **42**(9), 517–519 (2006).

#138060 - $15.00 USD Received 11 Nov 2010; revised 20 Dec 2010; accepted 25 Dec 2010; published 5 Jan 2011

15. F. Xu, and G. Brambilla, "Preservation of micro-optical fibers by embedding," Jpn. J. Appl. Phys. **47**(8), 6675–6677 (2008).
16. N. Lou, R. Jha, J. L. Domínguez-Juárez, V. Finazzi, J. Villatoro, G. Badenes, and V. Pruneri, "Embedded optical micro/nano-fibers for stable devices," Opt. Lett. **35**(4), 571–573 (2010).
17. G. M. Pajonk, "Transparent silica aerogels," J. Non-Cryst. Solids **225**(1), 307–314 (1998).
18. L. M. Xiao, M. D. W. Grogan, S. G. Leon-Saval, R. Williams, R. England, W. J. Wadsworth, and T. A. Birks, "Tapered fibers embedded in silica aerogel," Opt. Lett. **34**(18), 2724–2726 (2009).
19. H. Yokogawa, and M. Yokoyama, "Hydrophobic silica aerogels," J. Non-Cryst. Solids **186**, 23–29 (1995).
20. M. Sumetsky, "How thin can a microfiber be and still guide light?" Opt. Lett. **31**(7), 870–872 (2006).
21. N. Leventis, I. A. Elder, D. R. Rolison, M. L. Anderson, and C. I. Merzbacher, "Durable Modification of Silica Aerogel Monoliths with Fluorescent 2,7-Diazapyrenium Moieties. Sensing Oxygen near the Speed of Open-Air Diffusion," Chem. Mater. **11**(10), 2837–2845 (1999).
22. Y. L. Hoo, W. Jin, C. Z. Shi, H. L. Ho, D. N. Wang, and S. C. Ruan, "Design and modeling of a photonic crystal fiber gas sensor," Appl. Opt. **42**(18), 3509–3515 (2003).
23. A. van Brakel, C. Grivas, M. N. Petrovich, and D. J. Richardson, "Micro-channels machined in microstructured optical fibers by femtosecond laser," Opt. Express **15**(14), 8731–8736 (2007).
24. A. Roig, E. Molins, E. Rodríguez, S. Martínez, M. Moreno-Mañas, and A. Vallribera, "Superhydrophobic silica aerogels by fluorination at the gel stage," Chem. Commun. (Camb.) **20**(20), 2316–2317 (2004).
25. T. Y. Wei, S. Y. Lu, and Y. C. J. Chang, "Transparent, hydrophobic composite aerogels with high mechanical strength and low high-temperature thermal conductivities," J. Phys. Chem. B **112**(38), 11881–11886 (2008).
26. C. A. Morris, M. L. Anderson, R. M. Stroud, C. I. Merzbacher, and D. R. Rolison, "Silica sol as a nanoglue: flexible synthesis of composite aerogels," Science **284**(5414), 622–624 (1999).
27. M. K. Yang, R. H. French, and E. W. J. Tokarsky, "Optical properties of Teflon AF amorphous fluoropolymers," J. Micro/Nanolith. MEMS MOEMS **7**(3), 033010 (2008).
28. T. Bellunato, M. Calvi, C. Matteuzzi, M. Musy, D. L. Perego, and B. Storaci, "Refractive index dispersion law of silica aerogel," Eur. Phys. J. C **52**(3), 759–764 (2007).

1. Introduction

Optical nanofibres confine light to a small core, with strong evanescent fields and high optical nonlinearity [1–5]. Their advantages over other optical nanowires (such as silicon-on-insulator or chalcogenide strip waveguides) include built-in transitions to single-mode fibres with low coupling loss, extremely low optical loss (down to ~0.001 dB/mm) [4,5], high mechanical strength [6] and simplicity of fabrication [3–6]. A wide range of applications have been explored such as optical sensors [7,8], nanofibre circuits [3,9,10], nonlinear optics including supercontiuum generation [5,11] and high-Q resonators [4,12,13]. Unfortunately, their optical performance quickly degrades after fabrication due to surface light scattering from dust particles and from cracks induced by water vapour, resulting in large irrecoverable increases in loss and eventual mechanical failure [6,13–16]. The high surface-to-volume ratio and strong evanescent field of nanofibres make them particularly prone to this problem [4,14]. Couplers and resonators based on loops, coils or knots are also susceptible to mechanical disturbance because they are held in place only by weak natural adhesive forces.

Suspension in a hermetically-sealed package (as used to house fused fibre couplers) excludes dust and moisture but is not enough to stabilise looped devices and precludes sensing applications. Better support can be achieved on a low-index substrate such as MgF_2 [10] or silica aerogel [9], or between two such substrates [4], but these do not eliminate movement or ingress of moisture. Encapsulation in polymers such as Teflon (PTFE) [7,13–16] protects and stabilises nanofibres but at the expense of greatly increased attenuation (~2 dB/mm for 900 nm diameter [15] and 0.4 dB/mm for 1000 nm diameter [16] nanofibres at 1550 nm wavelength). Because the medium surrounding the nanofibre is an integral part of the waveguide, the high refractive index of the encapsulant (e.g. Teflon, $n = 1.31$) relative to air weakens light confinement, completely changes chromatic dispersion (and hence nonlinear properties), enhances the spread of the evanescent field and modifies the splitting properties of directional couplers, making it difficult to realise compact devices [7,13,15]. Encapsulation also prevents evanescent sensing, unless the encapsulant is thinned to allow the evanescent field to reach the external medium [7,16].

We overcome these drawbacks by embedding nanofibres in transparent hydrophobic silica aerogel formed in situ around the fibre using sol-gel chemistry [17,18]. Silica aerogel is nanoporous silica glass structured on a scale much smaller than optical wavelengths [17]. It has a low refractive index (typically 1.01 - 1.05), behaves optically like "solid air", and so has

#138060 - $15.00 USD Received 11 Nov 2010; revised 20 Dec 2010; accepted 25 Dec 2010; published 5 Jan 2011

little effect on the optical properties of nanofibre devices when replacing air around them. In particular, the optical attenuation due to encapsulation is much smaller with aerogel than with polymers. Aerogel is also thermally compatible with nanofibres, unlike polymers, because both are made from silica glass. Completely encapsulating a nanofibre in hydrophobic aerogel (rather than laying the nanofibre on the aerogel [9]) mechanically stabilises and protects the nanofibre from degradation, while the aerogel's porous structure allows the evanescent sensing of gases without exposing the bare nanofibre.

2. Method and applications

We have previously demonstrated the encapsulation of tapered fibres with diameters ≥1 μm in silica aerogel, and the induced loss was ~0.11 dB/mm [18]. However aerogel made by supercritical CO_2 drying is hydrophilic because its large-area internal surface is covered with hydroxyl groups as shown in Fig. 1(a) [19]. It can therefore condense water vapour from the air which can cause shrinkage under capillary forces. Indeed a drop of water quickly destroys the transparent aerogel where it lands, turning it to opaque white powder, Fig. 1(c). Hence the aerogel is not stable and we had to store our previous samples [18] in desiccant boxes. It was not then possible to similarly encapsulate submicron tapered fibres because the aerogel shrunk by ~4% during formation, which broke thinner fibres.

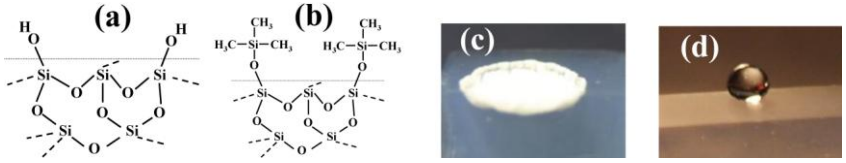

Fig. 1. Schematic internal surface structures of (a) hydrophilic aerogel with hydroxyl groups and (b) hydrophobic aerogel with trimethylsilyl groups. The horizontal lines distinguish the surface groups above from the bulk glass below. (c) Hydrophilic aerogel is turned to white powder by a 2.6 mm diameter drop of water. (d) A similar water drop sits without reacting on the surface of hydrophobic aerogel with a contact angle of ~160°.

In this work, to make the aerogel hydrophobic and avoid these problems we started with the same procedure as before, tapering low-loss (<0.1 dB) nanofibres and immersing them in a sol made from tetramethyl orthosilicate, methanol and water with ammonia as a catalyst [18]. After a few minutes the fluid sol around the nanofibre turns to rigid wet gel, which is aged for at least two days to allow the reaction to complete, then soaked in methanol for another two days to diffusively remove excess water. We then soaked the wet gel in 20 wt-% hexamethyldisilazane (HMDS) solution in methanol for a day to replace most surface hydroxyl groups with trimethylsilyl (-$OSi(CH_3)_3$) [17,19], as shown in Fig. 1(b). Importantly, we expect hydroxyl on the surface of the nanofibre to also be replaced, making the nanofibre itself hydrophobic too. Then the wet gel was soaked again in pure methanol to diffusively remove excess HMDS. The alcogel was immersed in liquid CO_2 (85 bar, ~20 °C) for 3.5 hours to diffusively replace the methanol within the gel, then the CO_2 was raised to supercritical conditions (100 bar, ~40 °C) for 2.5 hours, followed by depresssurisation over ~3 hours. This supercritically dries the wet gel to produce a block of hydrophobic aerogel with the nanofibre embedded in it. The aerogel made this way shrunk less than 1% in linear dimensions during formation and so did not damage the embedded nanofibre. This is a key beneficial side effect of the hydrophobic process. It was stable over time and waterproof, supporting a drop of water (without degradation) with a contact angle of 140 - 160°, Fig. 1(d). The aerogel was substantially transparent. Similar aerogel (without embedded fibres) had an attenuation of 0.02 dB/mm for 1550 nm light, and its refractive index was 1.05 as determined by measuring the critical angle for an internally-reflected laser beam. Samples have also been left floating in water for several months without apparent degradation.

Figure 2(a) shows a nanofibre waist 20 mm long and 0.8 μm in diameter embedded in hydrophobic aerogel. Figure 2(b) and 2(c) are scanning electron micrographs (SEMs) of tapered fibres emerging from aerogel blocks, showing the intimate contact between fibre and

#138060 - $15.00 USD Received 11 Nov 2010; revised 20 Dec 2010; accepted 25 Dec 2010; published 5 Jan 2011

aerogel. Figure 2(d) is a spectrum of the loss due to encapsulation for the fibre of Fig. 2(a). A reference transmission spectrum was measured through a length of fibre connected between a stable multiple-LED light source and an optical spectrum analyser. The fibre was then broken in the middle without disturbing the connections to the instruments, and the encapsulated sample was spliced into the fibre with a fusion splicer. A device transmission spectrum was then measured and divided by the reference measurement to yield a normalised loss spectrum. The measurement therefore includes the initial loss of the tapered fibre and of the two splice joints, and so is an upper bound for the loss due to encapsulation. (The total loss of the two splice joints was less than 0.1 dB.) The encapsulation loss divided by the length of the tapered waist was less than 0.03 dB/mm except around the OH peak at ~1380 nm, over an order of magnitude less than the lowest previously-reported attenuation for a Teflon encapsulated nanofibre [16] despite the smaller diameter.

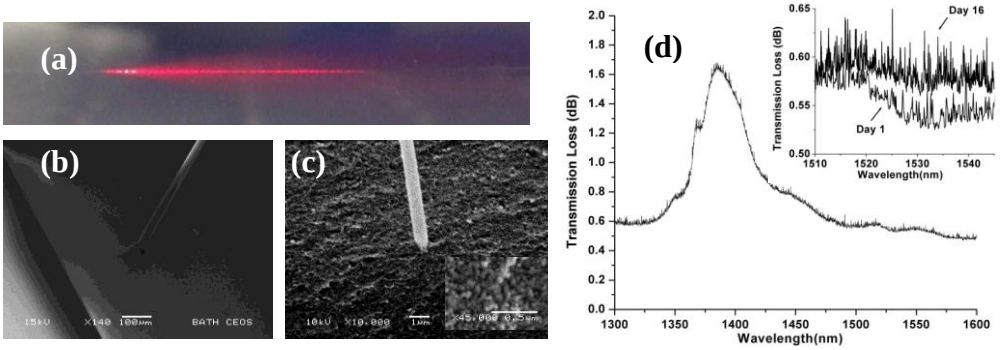

Fig. 2. (a) A nanofibre 20 mm long and 800 nm in diameter embedded in hydrophobic aerogel. The fibre carries red laser light from left to right, to reveal the nanofibre waist by the weak scattering of the evanescent field by the aerogel. Scanning electron micrographs (SEMs) of nanofibres with diameters of (b) 28 μm and (c) 700 nm emerging from aerogel blocks that were broken to show the intimate contact between fibre and aerogel. Inset: SEM of an aerogel surface (500 nm scale bar) with pore structure small compared to optical wavelengths. (d) The loss spectrum of the nanofibre immediately after encapsulation. Inset: detail between 1510 and 1545 nm immediately after encapsulation and 15 days later.

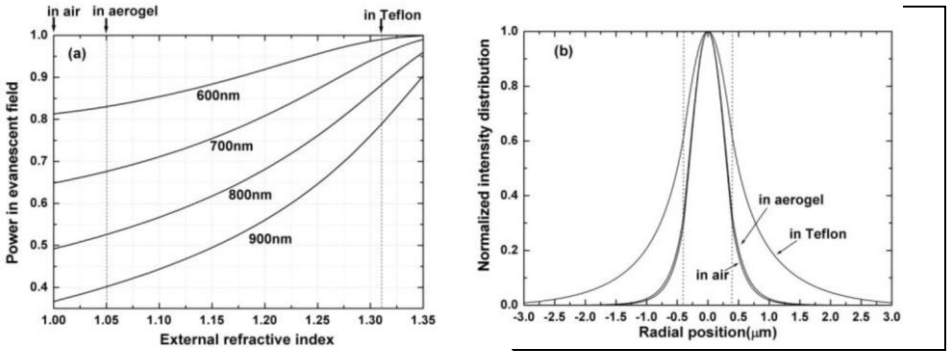

Fig. 3. (a) Calculated fraction of power in the fundamental mode's evanescent field at 1550 nm wavelength versus external index, for the nanofibre diameters marked. (b) Corresponding intensity distributions (normalised to a common peak value) along an axis perpendicular to the direction of the electrical field, for an 800 nm diameter nanofibre in air, aerogel and Teflon. The dotted lines mark the boundary of the nanofibre.

We attribute the lower attenuation mainly to stronger mode confinement by the low air-like refractive index of the aerogel (n = 1.05), as well as to its transparency. The fraction of fundamental mode power in the evanescent field is plotted in Fig. 3(a) against external index n. Light confinement in a 800 nm diameter nanofibre is similar with aerogel (n = 1.05) and air (n = 1.00) outside the nanofibre, but much weaker with Teflon (n = 1.31) and weaker still with

#138060 - $15.00 USD Received 11 Nov 2010; revised 20 Dec 2010; accepted 25 Dec 2010; published 5 Jan 2011

higher-index polymers, Fig. 3(b). Much less light therefore propagates in the lossier external medium and at the scattering fibre boundary. Another benefit is that the taper transition length needed for adiabatic propagation is much shorter [20].

The attenuation of the 800 nm encapsulated nanofibre was stable over time, changing by less than the ± 0.1 dB experimental error after 15 days' exposure to air in a lab without air conditioning or filtration, Fig. 2(d) inset. The attenuation of a narrower (700 nm diameter) encapsulated nanofibre did not change after two months. It is notable that the aerogel protects the nanofibre despite its open network of pores tens of nm wide. Though these are narrow enough to filter dust particles, water vapour can still diffuse into the aerogel and approach the nanofibre surface. However, any trimethylsilyl groups covering the nanofibre (from the process that made the aerogel hydrophobic) protect it from water adsorption and condensation, inhibiting the formation of the surface cracks thought to cause loss (and indeed mechanical weakness) [14–16].

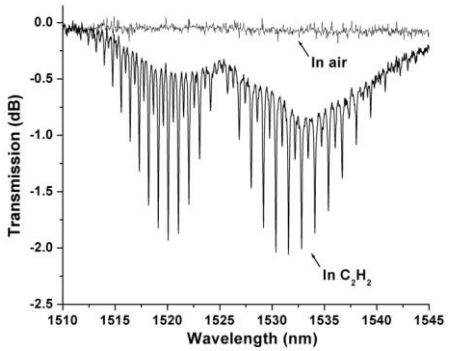

Fig. 4. Steady-state transmission spectra of a nanofibre with waist length 20 mm and diameter 800 nm embedded in aerogel, after the surrounding air was replaced by acetylene gas at atmospheric pressure, and after the acetylene was replaced by air again. The spectra are both relative to the transmission before the acetylene was first introduced.

Uniquely among proposed encapsulants, porous aerogel allows an embedded nanofibre to act as an evanescent-field gas sensor. Oxygen was reported to diffuse through aerogel at a rate only an order of magnitude slower than unimpeded diffusion in air, with a diffusion coefficient of 1-2 mm^2/s [21]. Acetylene (C_2H_2) has a conveniently-distinctive absorption spectrum, and should diffuse similarly in our aerogel because the gases' molecular masses and the aerogels' pore sizes are similar. We therefore demonstrated gas sensing by placing the encapsulated nanofibre of Fig. 2(a) in a test chamber into which acetylene gas could be introduced and removed at atmospheric pressure. The familiar absorption signature of acetylene appeared in the transmission spectrum, Fig. 4, increasing with concentration to a peak of ~2 dB at close to 100% concentration. The change was completely reversible, the induced loss returning to zero when the acetylene was removed. The response time was 16 ± 3 s for diffusion in both directions, consistent with the estimated diffusion time through 5 mm of aerogel [21]. The sensitivity can be increased by lengthening or narrowing the nanofibre, and the response speed by reducing the width of the aerogel block. The response time compares favourably with that of "holey" photonic crystal fibres, where the long diffusion distance severely increases the response time to over 3 hours for a 1 m fibre [22]. Micro-channels through the sides of the PCF speed up diffusion but need protection by a permeable material to prevent contamination while allowing gases to pass [22,23]. In contrast, the aerogel allows gases to diffuse directly to the nanofibre while blocking contaminants. Indeed the tendency of water droplets to roll off hydrophobic surfaces like our aerogel, collecting surface contaminants as it goes, is a "self-cleaning" property that could be useful in some applications [24].

For nonlinear-optical applications of nanofibres [5,11], the low air-like refractive index of aerogel is particularly valuable. Replacing air with aerogel has little effect on the nanofibre's

#138060 - $15.00 USD Received 11 Nov 2010; revised 20 Dec 2010; accepted 25 Dec 2010; published 5 Jan 2011

group-velocity dispersion spectrum (Fig. 5(a)) or the effective area of the guided mode (Fig. 3(b)), whereas both are very different in Teflon. Figure 5(a) shows that our nanofibre's zero-dispersion wavelength (a key parameter in nonlinear optics) is 510 nm in air and 530 nm in aerogel, whereas in Teflon the dispersion is always strongly normal and never zero. We could therefore demonstrate visible single-mode supercontinuum generation (Fig. 5(b)) in a 20 mm long nanofibre pumped by a pulsed green laser, as in [5] but with hydrophobic aerogel to protect the nanofibre and indefinitely extend its lifetime. The output spectrum was unchanged after half an hour, whereas an unencapsulated nanofibre would have been destroyed in this time by laser-induced heating at surface scatter points caused by dust or cracks.

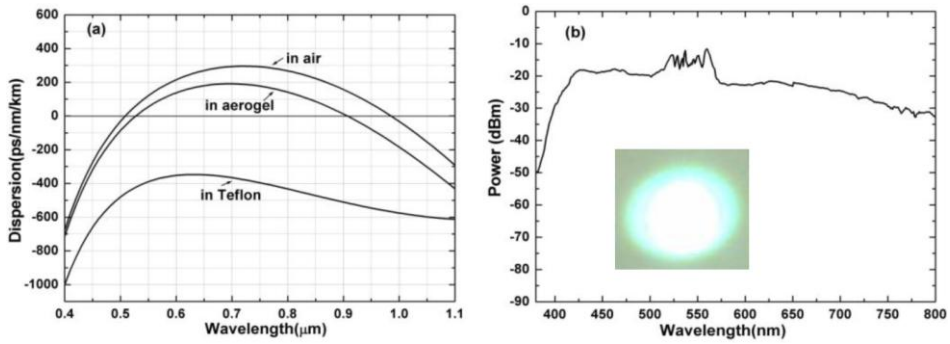

Fig. 5. (a) Calculated dispersion spectra of a silica nanofibre of diameter 800 nm in air, aerogel and Teflon. The material dispersion of silica and Teflon [27] are included, but that of aerogel was ignored because its index variation with wavelength is small compared to bulk silica [28]. (b) The output supercontinuum spectrum from a nanofibre 20 mm long and 800 nm in diameter embedded in aerogel, pumped by ~300 fs pulses of 540 nm wavelength with a repetition rate of 20 MHz. The total output power measured with a thermal power meter was 5.7 mW. Inset is a photograph of the output far field pattern.

Like other glass bodies, aerogel blocks are brittle and can be destroyed by rough treatment. Nevertheless our relatively dense (0.24 g/cm^3) aerogel was robust enough to be handled normally without damaging either the aerogel or the nanofibre inside it, with scope for further improvement [25]. Indeed the rigidity of this brittle encapsulant provides optical stability under mechanical or thermal stresses. All that is needed is a ruggedised secondary package to prevent gross crushing. We also expect aerogel-encapsulated devices to be more robust than the alternatives in high-pressure or vacuum environments, especially where the pressure is variable, because the aerogel allows gases around the nanofibre to "breathe" through the encapsulant.

3. Conclusion

In conclusion, encapsulation in hydrophobic aerogel overcomes key impediments to the exploitation of optical nanofibres and nanofibre devices, including degradation over time, encapsulation-induded loss, undesirable changes in light confinement and dispersion, thermal sensitivity, and movements in unsupported structures. The aerogel is a rigid barrier to particulate contaminants, waterproof on macroscopic and molecular scales, potentially self-cleaning, permeable to gases, and optically like air. We have demonstrated some of these improvements with a gas sensor and a supercontiuum source. It should also be possible to exploit other optical properties of the aerogel itself, including the ability to functionalise it with dopants [26].

Acknowledgements

The authors thank P. Reddish, Y. H. Yap, N. Wheeler, P. Mosley, and M. Rollings for useful discussions. This work is funded by the UK Engineering and Physical Sciences Research Council (EPSRC). T. A. Birks thanks the Leverhulme Trust for a Research Fellowship.

#138060 - $15.00 USD Received 11 Nov 2010; revised 20 Dec 2010; accepted 25 Dec 2010; published 5 Jan 2011